Phase transformation of PbSe/CdSe nanocrystals from core-shell to Janus structure studied by photoemission spectroscopy

J. Habinshuti,[1,2] P. Capiod,[1] T. H. Nguyen,[1] Y. Justo,[3] F. J. Avila,[4] M. C. Asensio,[4] F. Bournel,[5] J.-J. Gallet,[5] I. Vobornik,[6]
J. Fujii,[6] A. Addad,[7] K. Lambert,[3] J. P. Nys,[1] Y. Lambert,[1] Z. Hens,[3] A. Osherov,[8] Y. Golan,[8] O. Robbe,[9]
S. Turrell,[2] and B. Grandidier[1,*]

[1]*Département ISEN, Institut d'Electronique et de Microélectronique et de Nanotechnologies (IEMN), (CNRS, UMR 8520),*
41 Boulevard Vauban, 59046 Lille Cédex, France
[2]*Laboratoire de Spectrochimie Infrarouge et Raman (LASIR), Université des Sciences et Technologies de Lille,*
Bâtiment C5, 59655 Villeneuve d'Ascq Cedex, France
[3]*Physics and Chemistry of Nanostructures, Ghent University, Krijgslaan 281-S3, B-9000 Ghent, Belgium*
[4]*Synchrotron SOLEIL-Beamline ANTARES, 91192 Gif sur Yvette Cedex, France*
[5]*Laboratoire de Chimie Physique-Matière et Rayonnement (LCPMR), (CNRS UMR7614),*
11 rue Pierre et Marie Curie, 75231 Paris Cedex 05, France
[6]*INFM-CNR-TASC Laboratory, Area Science Park, Basovizza, I-34012 Trieste, Italy*
[7]*Laboratoire de Structure et Propriétés de l'Etat Solide, Université des Sciences et Technologies de Lille, 59655 Villeneuve d'Ascq, France*
[8]*Department of Materials Engineering, Ilse Katz Institute for Nanoscience and Nanotechnology,*
Ben-Gurion University of the Negev, Beer-Sheva 84105, Israel
[9]*Laboratoire de Physique des Lasers, Atomes et Molécules (CNRS, UMR 8523), Bâtiment P-5,*
Université des Sciences et Technologies de Lille, 59655 Villeneuve d'Ascq Cedex, France

Photoelectron spectroscopic measurements have been performed, with synchrotron radiation on PbSe/CdSe heteronanocrystals that initially consist of core-shell structures. The study of the chemical states of the main elements in the nanocrystals shows a reproducible and progressive change in the valence-band and core-level spectra under photon irradiation, whatever the core and shell sizes are. Such chemical modifications are explained in light of transmission electron microscopy observations and reveal a phase transformation of the nanocrystals: The core-shell nanocrystals undergo a morphological change toward a Janus structure with the formation of semidetached PbSe and CdSe clusters. Photoelectron spectroscopy gives new insight into the reorganization of the ligands anchored at the surface of the nanocrystals and the modification of the electronic structure of these heteronanocrystals.

I. INTRODUCTION

Irradiation of nanomaterials with energetic particles has been shown to produce significant changes in the material properties. Not only can point defects be created,[1–3] but also when the electron or ion energies increase, extensive amounts of materials can be displaced, leading to significant structural and chemical modifications.[4–6] For example, electron irradiation produces unusual mechanical changes because the reformation of chemical bonds considerably alters the plasticity of nanomaterials.[7,8] By increasing the electron energy that is released to an atomic lattice, even more fascinating structural changes have been obtained: Metal-tipped semiconductor nanorods have been converted into shell-like structures, for instance.[9,10] Irradiated nanomaterials, thus, provide an interesting playground for studying how direct atomic displacements and electronic excitations lead to the formation of defects, chemical disordering, phase segregation/ordering, or spinodal decomposition, in an effort to gain control over the fabrication of more and more complex nanostructures. Although radiation-induced phenomena can also be observed with intense fluxes in photons, the disordering effects are generally much reduced and are limited to the surfaces of the nanomaterials.[11–13] Through the use of spectroscopic techniques, light also offers the advantage of following the chemical changes that occur in nanoparticles

during a reaction.[14] Thus, it should give invaluable details into the kinetic pathways that exist when nanomaterials undergo radiation effects.

So far, the excitation of core-shell nanocrystals with synchrotron radiation has not revealed any chemical or morphological changes of these heteronanocrystals (HNCs) that would be induced by the photon beam.[15–17] In all cases, the synthesis of the shell corresponded to an epitaxial growth where the core and the shell materials were selected to crystallize in the same crystal structure. However, questions arise about the stability of HNCs that consist of two materials with different crystal structures and almost similar lattice constants. A typical system is the rocksalt PbTe/zinc-blende CdTe heterostructure where a mild annealing of a PbTe quantum well, that is embedded in a CdTe matrix, results in the formation of PbTe quantum dots.[18] Since PbSe/CdSe heterostructures have similar crystallographic properties and several studies have shown the benefit of using PbSe/CdSe core-shell HNCs to enhance the stability and the tunability of the optical properties of PbSe nanocrystals,[19,20] we investigated PbSe/CdSe heteronanocrystals with UV photoelectron spectroscopy based on synchrotron radiation. In contrast to HNCs with similar lattice types, we observed a reproducible modification of the valence bands and core levels for the main elements in the HNCs as a function of the irradiation time. By corroborating these findings with the structural transition

observed in transmission electron microscopy (TEM) when the HNCs are annealed *in situ*, we are able to rationalize the evolution of the signals originating from the different elements with respect to their chemical surroundings. Under light irradiation, the HNCs undergo a severe transformation from a core-shell structure toward a Janus structure that involves a dynamical exchange of the ligands between the initial CdSe surface of the HNCs and the emerging PbSe facets.

II. EXPERIMENTAL DETAILS

Oleate-capped PbSe core particles were synthesized according to literature methods.[21] The formation of a CdSe shell was achieved through a cationic exchange of Pb by Cd where a mixture of Cd oleate was added to the PbSe NC suspension in toluene heated at 100 °C.[22] In this reaction, Cd atoms replace the outermost Pb atoms in the nanocrystals, typically forming a CdSe shell around a PbSe core of reduced size. The sizes of the HNCs were controlled with optical spectroscopy and high-resolution-TEM. Six types of HNCs were prepared where the core diameter varied between 2.7 and 6.3 nm and the shell thickness varied between 0.6 and 2.0 nm.

In order to characterize the HNCs with UV photoelectron spectroscopy, Langmuir-Blodgett monolayers were formed by dropping the resulting HNCs, suspended in CHCl$_3$ on a Langmuir trough, followed by a single-stroke compression of the Langmuir film.[23] Transfers to gold-terminated Au-Si(111) surfaces were typically achieved at a surface pressure of 25 mN/m and were repeated two or three times. As a result, close-packed arrangements with a thickness of 2 to 3 monolayers were obtained over mm^2 areas. Such a thickness has been found to be enough to avoid any deleterious background signal from the gold surface in photoelectron spectroscopy of the valence band. Figure 1 shows a typical example of a gold-terminated surface covered with densely packed HNCs that was observed either with scanning electron microscopy (SEM) or with scanning tunneling microscopy. As PbSe nanocrystals are known to suffer from a reduction
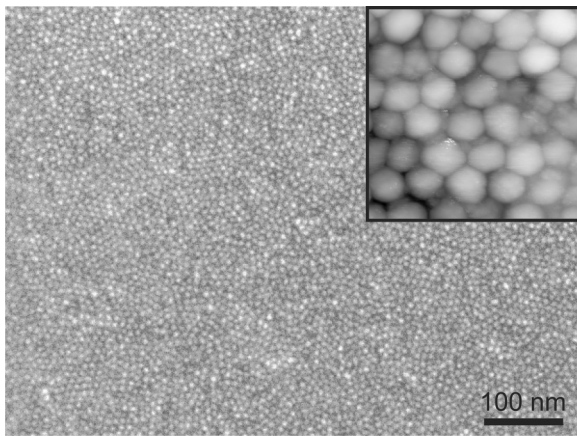

FIG. 1. Large-scale SEM image of PbSe/CdSe HNCs transferred by the Langmuir-Blodgett technique onto a gold-terminated Si(111) surface. Inset: high-resolution-STM image of the close-packed NC monolayer. The images were acquired at a sample voltage V_S of +2.0 V and a tunneling current I_t of 10 pA.

in the quantum yield with time due to the oxidation of the nanocrystal surface,[24] the samples were kept, as often as possible, in a vacuum vessel, in particular, during the transfer between the different experimental systems used for their characterization.

Photoelectron spectroscopic measurements were performed at beamline Antares at Soleil and beamline APE at Elettra. The synchrotron radiation was tuned in the energy range of 30–600 eV. A Scienta R4000 and a SES2002 analyzer were used to characterize the samples at room and low temperatures (between 75 and 110 K), respectively. High-energy resolution spectra of the valence bands and core levels were measured with a 5-eV pass energy, using either a single sweep or several sweeps to study the progressive changes in the core-level intensities caused by the irradiation. Since we worked with gold surfaces covered with only 1–3 monolayers of HNCs, the samples were not subject to charging effects. The binding-energy scale was calibrated using either the Fermi edge of gold-terminated areas that were not covered with HNCs on the samples or the Fermi edge of a clean and well-ordered Au reference sample. The core-level line shapes were fitted with Gaussian-Lorentzian convolution functions after standard background subtraction. The number of core-level components used in the fits was kept to a minimum and, in order to perform reliable decompositions, the broadening for the Gaussian and Lorentzian functions was calibrated from the measurements of core-level spectra obtained with bulk PbSe and CdSe materials. To this end, single-crystal PbSe films were epitaxially grown on GaAs substrates by chemical solution deposition as described in Ref. 25. Thick layers of zinc-blende CdSe were also grown by molecular-beam epitaxy on ZnTe and InAs substrates.[26]

In order to obtain valuable chemical information on the structure of the HNCs, in particular, close to the surface and the interface, the photon energy was predominantly set at 90–95 eV. Within this range of energies, the electrons have the shortest inelastic mean-free path of about 1 nm. In addition, such a low photon energy fits quite well with the binding energy of a few core levels of the three main elements in the HNCs: the Pb 5d, Se 3d, and Cd 4d core levels. It also ensures a high-energy resolution in order to distinguish the different chemical states of an element.

High-resolution TEM was performed using a FEI TECH-NAI G2 20 microscope operating at 200 kV that was equipped with a heating stage. The HNCs were deposited on a SiN TEM grid by drop casting suspensions in toluene, yielding arrays of 1 or 2 HNC monolayers. As the HNCs were found to be sensitive to the electron beam after some exposure, the TEM images had to be quickly acquired. During the *in situ* heating, only the final result was observed since the stabilization of the temperature on the grid usually takes a few minutes.

III. RESULTS

A. As-grown heteronanocrystals

We first start the description of the photoemission spectra with the measurement of the valence-band maximum (VBM) for bulk and nanocrystal materials. As shown in Fig. 2, the
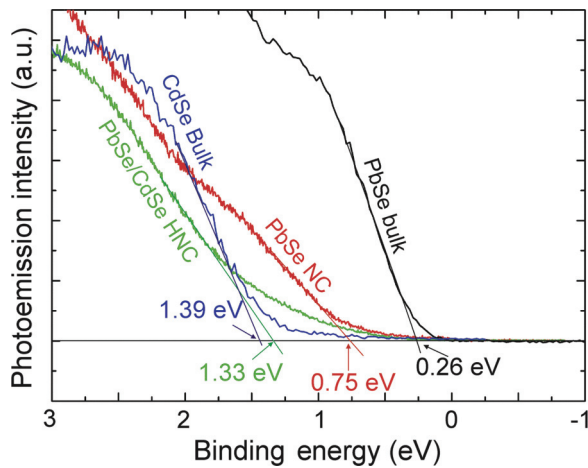
FIG. 2. (Color online) Valence-band photoemission spectra of bulk PbSe, PbSe nanocrystals (diameter: 9.3 nm), PbSe/CdSe hetero-nanocrystals (core sizes: 5.3 nm and shell thicknesses: 2.0 nm), and bulk CdSe. The photon energy was set at 95 eV, and the measurements were performed at room temperature. The valence-band maximum for each material is given and is determined by linear extrapolation of the leading edges.

position of the VBM was determined by a linear extrapolation of the valence-band spectrum from the high-energy edge to zero intensity. For bulk PbSe and bulk CdSe, we measure the VBM at 0.26 and 1.39 eV below the Fermi level, respectively. Such results are consistent with the value of bulk PbSe and CdSe band gaps at room temperature [0.28 eV (Ref. 27) and 1.73 eV (Ref. 28)] and are similar to the results found by photoemission spectroscopy for bulk CdSe in earlier studies.[29,30] They show that both materials have an *n*-type behavior and suggest the existence of a large valence-band discontinuity in PbSe/CdSe heterostructures since the VBM difference is 1.13 eV, slightly higher than the one that is found in the literature.[31] Such a result is consistent with the evidence for a quasi-type-II band alignment in PbSe/CdSe HNCs.[32] As to the PbSe nanocrystals with a diameter of 9.3 nm, the VBM shifts away from the Fermi level with respect to the bulk PbSe valence-band maximum. It lies 0.75 eV below the Fermi level at room temperature and, when the measurement is performed at 75 K, we find an upward shift, consistent with the temperature dependence of the PbSe band gap,[33] yielding a VBM positioned 0.52 eV below the Fermi level. Comparison with the theoretical band gap of 0.47 eV, calculated for a temperature of 0 K, reveals that the VBM shift observed for the PbSe nanocrystals is caused by quantum confinement.[34]

When the outermost Pb atoms are replaced with Cd atoms to turn the PbSe nanocrystals into PbSe/CdSe HNCs, the spectroscopic measurement also shows a shift in the VBM away from the Fermi level. Despite the increase in quantum confinement in the core, since the PbSe core diameter measures 5.3 nm instead of 9.3 nm, we do not attribute this stronger shift, in comparison with the one obtained for PbSe nanocrystals, to quantum confinement. Indeed, the shell is expected to be thicker than the escape depth of the photoexcited electrons. In addition, the theoretical band gap of a PbSe nanocrystal with a 5.3-nm diameter at 0 K is 0.75 eV,[34] a value significantly
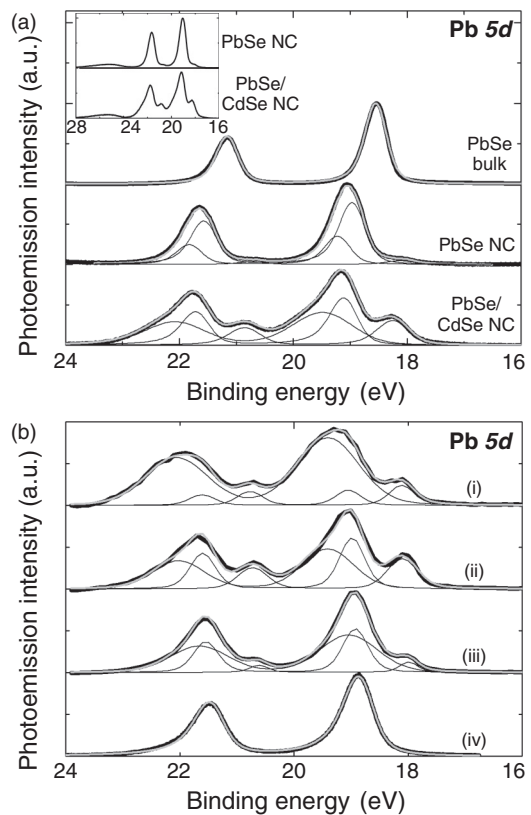

FIG. 3. (a) Background subtracted high-resolution Pb 5*d* core-level spectra of bulk PbSe, PbSe nanocrystals (diameters: 9.3 nm), and PbSe/CdSe heteronanocrystals (core sizes: 5.3 nm and shell thicknesses: 2.0 nm). The thin lines correspond to fits obtained with the parameters given in Table I. The photon energy was set at 95 eV. Inset: background subtracted Pb 5*d* core-level spectra of the PbSe nanocrystals and PbSe/CdSe heteronanocrystals observed on a wider energy range to show a broad and small peak around 25 eV. (b) Evolution of the line shape of the Pb 5*d* core level during the surface preparation of bulk PbSe. Spectrum (i) corresponds to a surface treated with a soft Ar sputtering, whereas, spectrum (iv) was measured after three cycles of sputtering and annealing. All spectra were measured at room temperature.

smaller than the measured energy of 1.33 eV, even though this value is measured at room temperature. Rather, this energy shift agrees well with a shell consisting of a material with a larger band gap than PbSe in agreement with the presence of pure CdSe or mixed $Pb_{1-x}Cd_x$Se.

In order to determine the chemical composition of the shell, we further analyze the core levels of the four types of materials described in this paper, beginning with the measurements of the core levels for the bulk PbSe and CdSe materials. Figures 3(a), 4 and 5 show the Pb 5*d*, Se 3*d*, and Cd 4*d* photoelectron spectra of both materials. All spectra are composed of two peaks that are more or less separated due to the different magnitudes of the spin-orbit coupling for each element. A reasonable description of the spectra is obtained with only one component. The peak positions and the linewidth of the Gaussian and Lorentzian functions used to perform the decomposition are given in Table I. We find Lorentzian and Gaussian contributions to the Pb 5*d* level that agree with previous studies of bulk lead chalcogenides.[35,36] Similar to these past studies, we were not
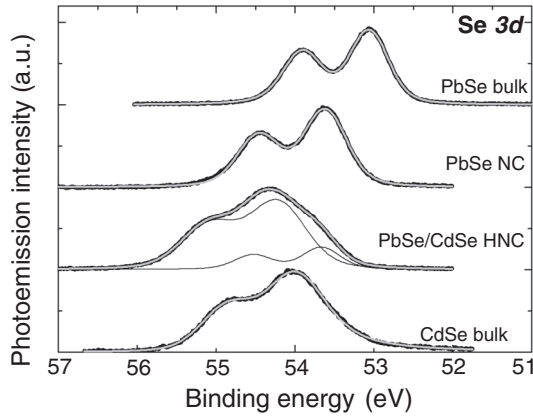
FIG. 4. Background subtracted high-resolution Se 3*d* core-level spectra of bulk PbSe, PbSe nanocrystals (diameters: 9.3 nm), PbSe/CdSe heteronanocrystals (core sizes: 5.3 nm and shell thicknesses: 2.0 nm), and bulk CdSe. The thin lines correspond to fits obtained with the parameters given in Table I. The photon energy was set at 95 eV, except for the characterization of bulk CdSe where it was 90 eV. All spectra were measured at room temperature.

able to discriminate between surface and bulk components of Pb atoms.

As to the linewidth, the spin-orbit splitting, and the branching ratio of the Se 3*d* levels in PbSe, all quantities are consistent with experimental results given in the literature and do not show the existence of a surface component.[37–40] This is also the case for the decomposition of the Cd 4*d* core level in CdSe. Although the Lorentzian function is rather on the broad side of the linewidths found in the literature, a single component fully describes the measured spectrum.[41–43] In contrast, we find that the Se 3*d* level in this material required a much larger broadening with respect to the Se 3*d* level in PbSe. Finally, we note a clear chemical shift of 1.02 eV between the Se components in PbSe and CdSe.

Interestingly, the preparation of a clean PbSe surface reveals additional components for the Pb 5*d* core level, that could be helpful in understanding the chemical states found in the HNCs. Starting from an oxidized PbSe surface, the surface was gently sputtered to reveal the Pb 5*d* core-level peaks as shown in spectrum (i) of Fig. 3(b). This spectrum consists of two broad peaks with two small shoulders at lower binding energies [spectrum (i)]. Increasing the number of
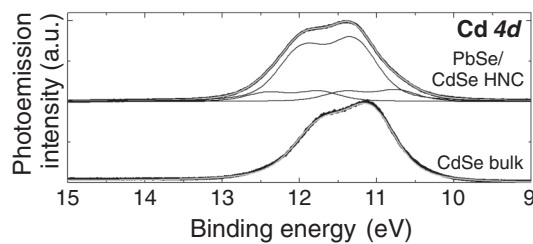

FIG. 5. Background subtracted high-resolution Cd 4*d* core-level spectra of PbSe/CdSe heteronanocrystals (core size: 5.3 nm and shell thickness: 2.0 nm) and bulk CdSe, obtained with photon energies of 95 and 90 eV, respectively. The thin lines correspond to fits obtained with the parameters given in Table I. Both spectra were measured at room temperature.

TABLE I. Fitting parameters of Figs. 2(a), 3, and 4.

Materials	Peak	Binding energy (eV)	Spin-orbit splitting (eV)	Gaussian FWHM (eV)	Lorentzian FWHM (eV)
PbSe bulk	Pb_1	18.55	2.61	0.31	0.20
	Se_1	53.04	0.84	0.45	0.20
PbSe NC	Pb_1	18.96	2.60	0.40	0.20
	Pb_2	18.14	2.60	0.47	0.20
	Pb_3	19.21	2.60	0.36	0.20
	Se_1	53.61	0.84	0.52	0.20
PbSe/CdSe	Cd_1	11.29	0.68	0.54	0.30
CS NC	Cd_2	10.74	0.68	0.46	0.30
	Cd_3	11.74	0.68	0.47	0.30
	Pb_1	19.05	2.60	0.40	0.20
	Pb_2	18.20	2.60	0.50	0.20
	Pb_3	19.41	2.60	1.08	0.20
	Se_1	53.67	0.86	0.45	0.20
	Se_2	54.30	0.86	0.60	0.54
CdSe bulk	Cd_1	11.07	0.66	0.55	0.39
	Se_2	54.06	0.85	0.64	0.55

sputtering and annealing cycles first increases the intensity of the shoulders [spectrum (ii)] but, eventually, leads to their disappearance [spectrum (iv)]. At the same time, the major peaks become narrower and narrower and shift toward lower and lower binding energies.

Fitting the different Pb 5*d* core-level spectra requires three doublets. The initial broad peak at high binding energies is known to be caused by oxidized Pb atoms at the surface.[44,45] With the removal of the oxide layer due to the sputtering, the spectral line becomes narrower revealing the $5d_{5/2}$ and $5d_{3/2}$ lines of the bulk components. As to the shoulders visible at low binding energies, they are attributed to Pb adatoms that are created due to the preferential sputtering of selenide ions.[46] Prolonged annealing allows them to be reintegrated in the surface lattice again, leading to the occurrence of a single doublet for the Pb 5*d* core level, once the surface is correctly prepared.

Based on the linewidths obtained for the bulk materials in this paper and the ones found in the literature, we can now investigate the chemical states of the nanocrystals. We first focus on the photoelectron spectra of PbSe nanocrystals with mean diameters of 9.3 nm. The Pb 5*d* and Se 3*d* core-level spectra are displayed in Figs. 3(a) and 4. The comparison of their positions with respect to the core levels of PbSe bulk reveals a significant shift toward higher binding energies that we attribute to a change in the material work function. Although one component is enough to fit the Se 3*d* core level, three components are necessary to get a good fit of the Pb 5*d* core level. These results are in line with our current understanding of the surface chemistry of PbSe nanocrystals capped with oleate.[47–49] Indeed, we know that the nanocrystals are nonstoichiometric with a surface that is predominantly composed of lead. Thus, we expect the Se 3*d* core level to mainly consist of a bulk component which is supported by the decomposition of the related spectrum. Conversely, due to the surface excess of Pb atoms, several components should account for the line shape of the Pb 5*d*

core level. We attribute the central peak with the highest intensity to the bulk component, whereas, both other peaks are related to the surface components. In fact, during the synthesis, oleate ligands are adsorbed at the lead-rich surface through oxygen atoms. In addition, if the nanocrystals are left in solution or are transferred in air, they can progressively oxidize. This is particularly true during the film preparation by the Langmuir-Blodgett method. Accordingly, we expect the contribution of the PbO species in the line shape of the Pb $5d$ level at high binding energies, yielding broad shoulders similar to the ones found at the beginning of the surface preparation of the PbSe bulk. In vacuum, annealing the nanocrystals between $100\,°C$ and $200\,°C$ is known to desorb part of the ligands.[50] As we cannot rule out that a partial desorption of weakly bound ligands occurs in ultrahigh vacuum, that could be enhanced by heating due to the intense flux in photons, we expect unbound excess Pb atoms at the surface of the PbSe nanocrystals. Such atoms, with more metallic characters, give another contribution to the line shape of the Pb $5d$ level at low binding energies, similar to the peak observed after the sputtering of the PbSe bulk surface. Therefore, fitting the Pb $5d$ with three components is consistent with the achieved decomposition and with the result described in a recent study.[49] Finally, we also notice a small peak at a binding energy around 25 eV [inset of Fig. 3(a)]. This peak is the signature of the O $2s$ core level that is caused by the O atoms of the ligands and/or the oxidation of the Pb species.

We now turn to the chemical state analysis of the HNCs that were directly synthesized from the parent PbSe nanocrystals described above. Although the PbSe core is expected to be covered with a shell thicker than the escape depth of the photoexcited electrons, we note that a significant signal is measured in the energy range of the Pb $5d$ core level. Moreover, marked changes are observed in the spectra of the three elements in comparison with the spectra measured for the parent nanocrystals as shown in Figs. 3–5. The line shape of the Pb $5d$ is clearly different. Although three components still give a reasonable description of the experimental spectrum, the intensity of the peaks that have been assigned to the surface components of the Pb core level are now much stronger. At first, the capping of the PbSe core with an inorganic shell of CdSe makes the observation of the Pb core level quite surprising since a 2-nm-thick shell should prevent the escape of electrons from the core at a photon energy of 90–95 eV. However, several experimental papers have shown that the core can have an off-center position in the final structure and that the shell is very often incomplete.[22,51,52] PbSe facets, thus, exist close to or at the surface of the HNCs, and the related Pb species contribute more strongly to the signal than the bulk component, for which the photoexcited electrons are more attenuated.

The existence of PbSe facets at the surface is corroborated by the line shape of the Se $3d$ core level (Fig. 4). Indeed, we were not able to fit the Se $3d$ spectrum of the HNCs with a single component based on the fitting parameters used for the CdSe bulk. Another component exists at a low binding energy, and we reasonably assign it to Se atoms residing in the PbSe part of the HNCs. The energy shift in this component is consistent with the difference in energy measured for the Se $3d$ core level between CdSe and PbSe bulk. The observation of such a component, thus, favors the existence of a partial

shell, allowing electrons to escape from the PbSe part of the HNCs.

Next, we consider the Cd $4d$ core level (Fig. 5). Again, the fitting parameters of the bulk were used and led to a decomposition with three components instead of the single one found for CdSe bulk. Likewise, for Pb, a central doublet is surrounded by two smaller doublets. We attribute this central doublet to the bulk component. In order to account for the other components, we know that Se gets oxidized before Cd when CdSe is subject to oxidation.[53,54] As we were not able to detect any additional peak at high binding energies in the Se $3d$ spectrum, we rule out a strong oxidation of Cd atoms at the surface of the shell. However, the synthesis involves the binding of these Cd atoms with oleic acid ligands through an oxygen atom. Based on previous photoelectron experiments, we attribute the contribution of these atoms to the component observed at the highest binding energy.[54,55] Regarding the component seen at the lowest binding energy, we could imagine that parts of the Cd atoms become unsaturated at the surface, for example, if Cd-O bonds are cleaved in ultrahigh vacuum. Similar to the excess of Pb atoms detected at the surface, such Cd atoms have a more metallic nature[55] and lead to the occurrence of a low binding energy component in the core-level spectrum.

Although the existence of additional components in the core-level spectra of Pb and Cd could be caused by the formation of an alloy structure,[49] we rule out this hypothesis. The lattice-type mismatch between rocksalt IV-VI semiconductors and zinc-blende II-VI semiconductors makes both materials very immiscible.[56] Although not impossible, the investigation of bulk $Pb_{1-x}Cd_xTe$ solid solutions by photoelectron spectroscopy, for a small content of Cd, did not display the existence of shoulders at low binding energies in the Pb $5d$ core-level spectrum.[57,58] Moreover, recent experiments have shown that ion exchange certainly proceeds in a layer-by-layer fashion, preventing a strong intermixing between Pb and Cd atoms.[59,60] Therefore, the well-resolved component seen on the Pb $5d$ core level at the lowest binding energy indicates that Pb exists in excess on the few PbSe facets at the surface of the HNCs and, possibly, on the CdSe surface of the shell. Such a hypothesis agrees with a recent study of the Pb $5d$ core-level spectrum measured for PbSe/CdSe HNCs with a complete shell that shows a shoulder at low binding energy, whereas, the PbO component was absent from the spectrum.[49] This result would suggest that Pb is not expulsed from the outer layer of the shell as fast as it was initially thought.

In order to confirm these observations, other HNCs were characterized. Their chemical-states analysis revealed that the line shapes of the Pb $5d$, Se $3d$, and Cd $4d$ core levels were quite reproducible for all six types of investigated HNCs. Figure 6 shows an example of the line shape obtained for the Pb $5d$ core levels of four different HNCs, and Table II gives the related parameters of the fits. In all spectra, the peak at low binding energy is clearly seen. When we compare its intensity as a function of the shell thickness, we are not able to find any strong dependence between the intensity of the line and the shell thicknesses. In the same way, changing the core diameter, while maintaining the shell thickness constant, does not greatly alter this peak.
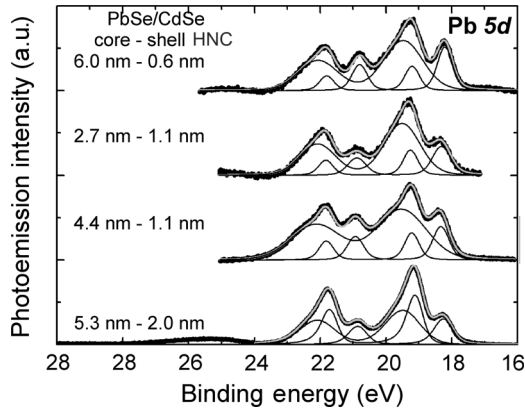
FIG. 6. High-resolution spectra Pb 5*d* core-level spectra of four PbSe/CdSe heteronanocrystals with their intended sizes given in front of each spectrum. The thin lines correspond to fits obtained with the parameters given in Table II. The spectra were measured at 110 K.

FIG. 7. (Color online) Survey spectra of PbSe/CdSe hetero-nanocrystals obtained in normal emission with a photon energy of 95 eV. Initially, the core size of the heteronanocrystals is 4.4 nm, and the shell thickness is 1.1 nm. The lower (i), middle (ii), and upper (iii) spectra correspond to a fresh sample, the same sample annealed at 130 °C for 30 min and after being irradiated for 2 h. The spectra were measured at 110 K.

B. UV-irradiated heteronanocrystals

Remarkably, the line shapes of the different core levels were found to reproducibly change when all six types of HNCs were annealed or were kept under the exposure of the photon flux. Figure 7 gives an example through survey spectra measured in the case of the HNCs having a core diameter and a shell thickness of 4.4 and 1.1 nm, respectively. Starting with spectrum (i) obtained for a fresh sample, a modification in the line shape of the Pb 5*d* core level is seen once the samples have been annealed at 130 °C for 30 min [spectrum (ii)]. The changes are more dramatic when the HNCs are exposed to irradiation for 2 h. Not only the peak at low binding energy in the Pb 5*d* core level tends to disappear, but the Se 3*d* becomes featureless, and a clear shift in the binding energy is visible for the Cd 4*d* core level.

In order to better highlight the chemical transformation of the HNCs caused by the fluxes in the photons, high-resolution spectra were acquired in the following manner. High-resolution spectra of the three different core levels were quickly measured on a sample that had not been annealed or had been subject to irradiation before. Then, because the change in the line shape is more pronounced for the Pb 5*d* level,
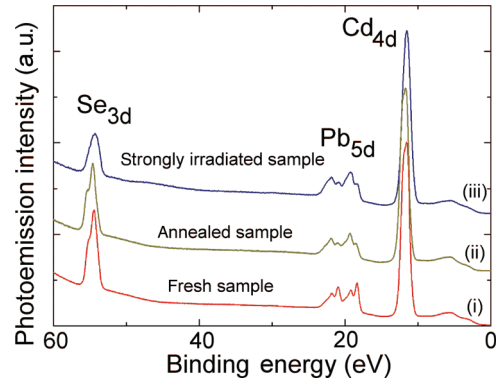
several sweeps were acquired for durations of tens of minutes in the energy range of the Pb 5*d* level. Finally, spectra of the Se 3*d* and Cd 4*d* core levels were again measured. Figure 8 shows a typical set of measurements with the related fits (the fitting parameters being tabulated in Table III). Initially, the first component of the Pd 5*d* core level at low binding energy has the strongest contribution with respect to the other components. At the same time, the Se 3*d* core level shows two lines with a major contribution of the Se element belonging to the CdSe shell. As for the Cd 4*d* core level, it is described with three components as already found for the HNCs described previously.

Under irradiation, the intensity of the different lines in the Pb 5*d* core levels changes. The intensity of the peak positioned at low binding energy clearly decreases, whereas, the contribution of the peak at the highest binding energy gets stronger and stronger. At the end of this continuous exposure, the line shape of the Se 3*d* core level is broader. When fitted, it shows a slight increase in the contribution of the Se element residing in PbSe. As far as the Cd element is concerned, a single component is necessary to fit the Cd 4*d* core level,

TABLE II. Fitting parameters of Fig. 6.

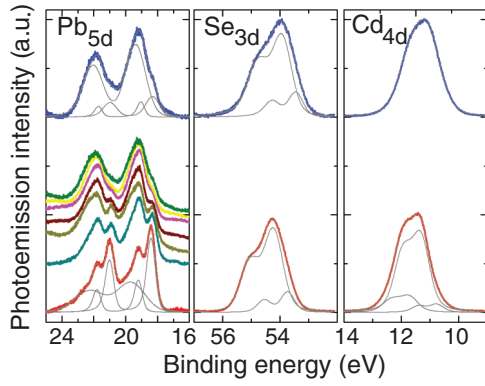| Materials core/shell (nm)/(nm)	Peak	Binding energy (eV)	Spin-orbit splitting (eV)	Gaussian FWHM (eV)	Lorentzian FWHM (eV)
6.0/0.6	Pb$_1$	19.19	2.59	0.40	0.20
	Pb$_2$	18.20	2.59	0.43	0.20
	Pb$_3$	19.46	2.59	1.28	0.20
2.7/1.1	Pb$_1$	19.25	2.57	0.40	0.20
	Pb$_2$	18.31	2.57	0.54	0.20
	Pb$_3$	19.51	2.57	1.16	0.20
4.4/1.1	Pb$_1$	19.21	2.60	0.40	0.20
	Pb$_2$	18.32	2.60	0.43	0.20
	Pb$_3$	19.53	2.60	1.60	0.20
5.3/2.0	Pb$_1$	19.05	2.60	0.40	0.20
	Pb$_2$	18.20	2.60	0.50	0.20
	Pb$_3$	19.41	2.60	1.08	0.20

FIG. 8. (Color online) Evolution of the high-resolution core-level spectra for the main elements in PbSe/CdSe heteronanocrystals under illumination at 95 eV. Initially, the characterized heteronanocrystals have core size of 4.4 nm and shell thickness of 1.1 nm. Lower spectra: beginning of the experiments; intermediate spectra: consecutive sweeps of the Pb core-level spectrum; upper spectra: end of the experiments. The thin lines correspond to fits obtained with the parameters given in Table III. The spectra were measured at 110 K.

based on the fitting parameters used for the Cd element in the zinc-blende CdSe bulk.

Although the core-level spectra of the three main elements are found to change, it is interesting to note that the O 2s core level barely changes. A good comparison is shown in Fig. 9 for the PbSe/CdSe HNCs (core size of 9.3 nm/shell thickness of 2.0 nm) and their parent PbSe nanocrystals. Comparison of spectra (i) and (ii), obtained for as-grown nanocrystals and nanocrystals exposed to irradiation for a few minutes, respectively, shows the typical reduction in the shoulder seen at the low binding energy in the Pb 5d core-level spectrum of the HNCs due to irradiation. However, there is no significant reduction in the broad peak related to the O 2s core level, indicating that the irradiation-induced modifications do not involve a desorption of the oleate.

Following the Pb 5d core-level changes, we were also able to measure variation in the valence band of the HNCs. The inset

TABLE III. Fitting parameters of Fig. 8.

| Time (min)	Peak	Binding energy (eV)	Spin-orbit splitting (eV)	Gaussian FWHM (eV)	Lorentzian FWHM (eV)
0	Cd$_1$	11.35	0.63	0.54	0.30
	Cd$_2$	10.77	0.63	0.39	0.30
	Cd$_3$	11.73	0.63	0.55	0.30
	Pb$_1$	19.14	2.60	0.42	0.20
	Pb$_2$	18.35	2.60	0.47	0.20
	Pb$_3$	19.58	2.60	1.94	0.20
	Se$_1$	53.73	0.82	0.45	0.20
	Se$_2$	54.23	0.82	0.64	0.22
120	Cd$_1$	11.04	0.65	0.76	0.38
	Pb$_1$	18.98	2.66	0.40	0.20
	Pb$_2$	18.24	2.66	0.86	0.20
	Pb$_3$	19.29	2.66	1.33	0.20
	Se$_1$	53.40	0.85	0.45	0.20
	Se$_2$	53.88	0.85	0.64	0.22
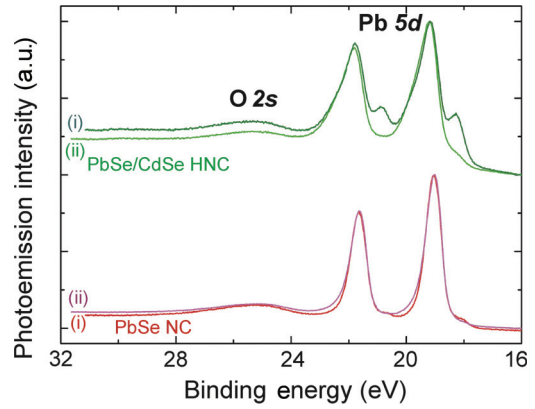
FIG. 9. (Color online) Evolution of the high-resolution Pb 5d and O 2s core-level spectra of PbSe nanocrystals (diameters: 9.3 nm) and PbSe/CdSe heteronanocrystals (core size: 5.3 nm and shell thickness: 2.0 nm) under illumination at 95 eV. Spectra (i) and (ii) correspond to a brief and longer illumination, respectively.

of Fig. 10 again shows the reduction in the shoulder seen at the low binding energy in the Pb 5d core-level spectrum when HNCs (core size of 4.4 nm/shell thickness of 1.1 nm) are slightly annealed [spectrum (ii)] or irradiated [spectrum (iii)]. The leading edge of the valence band clearly shifts toward a lower binding energy when the HNCs are subject to annealing or irradiations.

Therefore, the analysis of these results indicates:

(1) the disappearance of the CdO species along with a strong reduction in Pb and Cd atoms in excess,

(2) the emergence of PbSe facets at the surface that should be terminated with oleate ligands.

IV. DISCUSSION

In order to gain further insight into the transformation of the HNCs, the samples were observed with SEM after their irradiation (Fig. 11). The morphology of the film looks
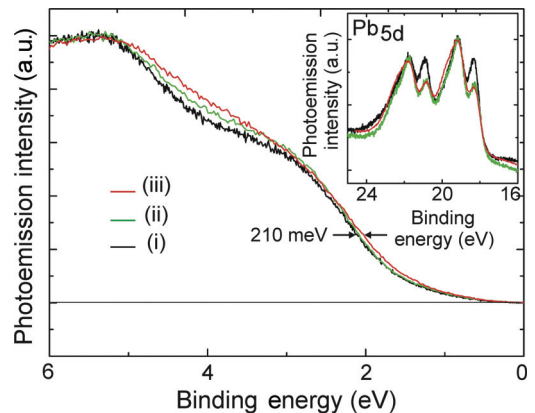

FIG. 10. (Color online) Photoemission spectra of the valence bands of heteronanocrystals with core sizes of 4.4 nm and shell thicknesses of 1.1 nm under illumination at 95 eV. The spectra were obtained (i) for as-grown HNCs, (ii) after a brief annealing and short irradiation time, and (iii) after an irradiation time of a few minutes. Inset: evolution of the related high-resolution Pb 5d core-level spectra. The spectra were measured at 110 K.
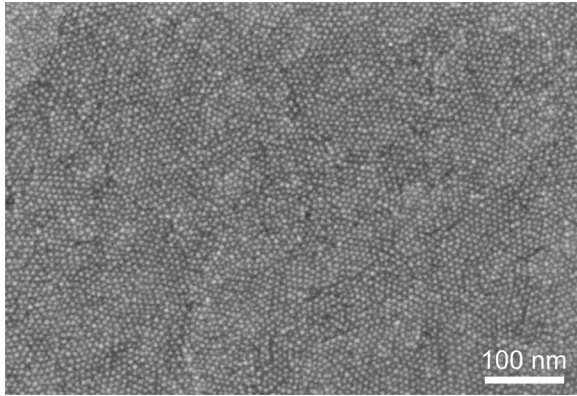
FIG. 11. Large-scale SEM image of PbSe/CdSe heteronanocrystals transferred by the Langmuir-Blodgett technique onto a gold-terminated Si(111) surface. The sample was observed after its characterization by synchrotron radiation. The initial dimensions of the heteronanocrystals were: core diameter of 4.4 nm and shell thickness of 1.1 nm.

FIG. 13. TEM image of PbSe/CdSe heteronanocrystals after annealing the sample observed in Fig. 12 (200 °C for 15 min). The inset shows high-resolution-TEM images of a Janus-like heteronanocrystal.

similar to the one seen in Fig. 1. Individual HNCs are still clearly visible, and we were not able to detect any sign of fusion, leading to their subsequent attachment.[61] Therefore, the changes observed in photoelectron spectroscopy only involve an internal transformation. Since we noticed similar effects on the evolution of the core level when the samples are annealed or are exposed to UV irradiation, the HNCs were studied with TEM where they could be annealed *in situ* and their transformation could be followed in real time.
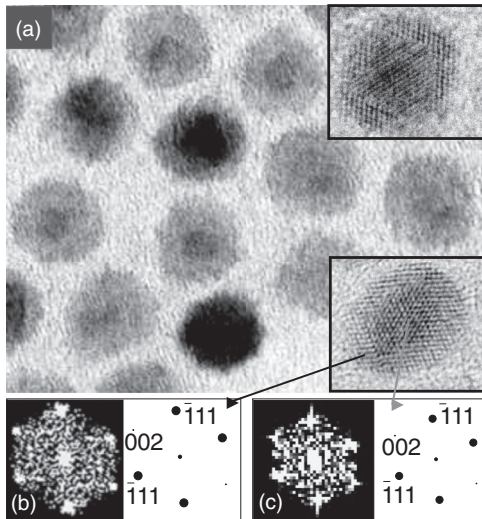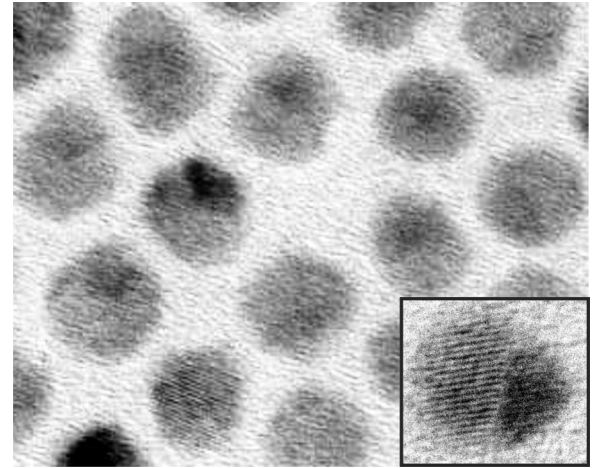

FIG. 12. TEM image of PbSe/CdSe heteronanocrystals with mean dimensions of 5.3 and 2.0 nm for the core size and the shell thickness, respectively. The top and bottom insets show high-resolution-TEM images of heteronanocrystals with partial shell and complete shell, respectively. (b) and (c) Fourier transforms of the shell and core regions that are pointed out in the high-resolution image of the heteronanocrystal with a complete shell and simulated electron-diffraction patterns for PbSe and CdSe crystals with rocksalt and zinc-blende structures, respectively.

Figure 12(a) shows TEM images of PbSe/CdSe HNCs obtained before annealing for nanocrystals with intended core size and shell thickness of 5.3 and 2.0 nm, respectively. The HNCs have a rather spherical shape. For a large majority of the HNCs, the core region can be distinguished from the shell due to a darker contrast. To illustrate the detailed atomic arrangement within a single nanocrystal, an enlarged high-resolution-TEM image of a HNC with a complete shell is shown in the lower inset of Fig. 12(a). Fast Fourier transformation of the atomic arrangement acquired in the core [Fig. 12(b)] and in the shell [Fig. 12(c)] yields diffraction patterns that match well with simulated (−1−10) patterns of rocksalt PbSe and zinc-blende CdSe, consistent with previous papers.[22,49,51] However, two types of HNCs are seen as follows: HNCs that are fully covered with a shell (lower inset) and HNCs where the core is partially embedded in a shell (upper inset).

When the HNCs are heated at 150 °C for a few minutes, morphological changes are usually observed for the nanocrystals with the thinnest shells. The transformation is quite clear around 200 °C for the majority of the HNCs as seen in Fig. 13. In this case, HNCs still show two regions. Based on their contrast and their expected volume, we identify the smallest and darkest one to be PbSe and the largest and brightest one to be CdSe. Remarkably, the transformation involves a disruption of the shell that leads to the expulsion of the core at the surface of the HNCs, the latter one conserving a rather spherical shape. High-resolution-TEM images clearly reveal the formation of a Janus structure where two bihemispheres are in contact, consistent with the results found by Grodzinska *et al.*[51]

From these observations, we can now draw the following interpretation of the evolution of the chemical states observed during photon irradiation. Upon thermal annealing, minimization of the interface energy has been shown to lead to a phase separation in the absence of lattice mismatch between similar compounds, such as PbTe and CdTe.[62] In the case of a PbSe core embedded in a CdSe matrix, the minimization of the total energy of the system occurs through the formation of

{111} interfaces between both compounds where a Se {111} layer separates the Pb and Cd sublattices.[60] For spherical core-shell nanocrystals where the volume of CdSe is limited, the reduction in the energy to reach a single {111} interface involves the expulsion of the core from the shell through atomic rearrangements. Such a transformation appears in the evolution of the Se $3d$ core-level spectrum where the contribution of the Se element bound to Pb becomes stronger. It is also seen in the change of the intensities for the components that compose the Pb $5d$ core-level spectrum. An increase in the contribution caused by Pb atoms bound to O implies the emergence of new facets at the surfaces of the HNCs.

Along with the disappearance of the CdO species and the lack of attachment and fusion of HNCs below 300 °C in the TEM images, this finding indicates that the ligands do not significantly desorb under irradiation, consistent with the stability of the O $2s$ core level. Heating due to irradiation is, thus, lower than 200 °C, a temperature that is still low enough to prevent the desorption of oleate ligands attached to Pb atoms at the surface of PbSe NCs.[63] Therefore, although Cd atoms in excess at the surface of the shell reintegrate in the CdSe lattice upon annealing, the ligands preferentially diffuse from the CdSe facets to the PbSe facets and bind to Pb adatoms. A possible alternative would be that excess Pb adatoms diffuse at the surface of the HNCs toward the CdSe facets and saturate the oleate ligands there. At the end of the transformation, a semiattached structure is obtained where the PbSe facets are stabilized with organic ligands. From the signature of the small component observed in the Pb $5d$ core level at the lowest energy, a small excess of Pb atoms still exists at the surface of the HNCs. We surmise that this excess of cation atoms certainly plays a significant role in favoring the diffusion of inorganic and organic elements during the phase transformation. Indeed, in contrast to these effects observed in vacuum, heating of colloidal suspensions of HNCs does not produce the same effect.[51]

Finally, the photoemission measurements of the valence band reveal that the morphological change takes place with a modification of the density of states in the valence band. A VBM shift in 210 meV toward the Fermi level is measured in Fig. 10. However, from the size of the PbSe core (4.4 nm) and its expected contribution into the signal measured at low energy when the HNCs are turned into a Janus structure, it is surprising to measure a VBM that is so far from the Fermi level. Indeed, although we cannot rule out a change in the Fermi

level pinning with the irradiation-induced transformation, the band gap of a PbSe NC with a size of 4.4 nm is predicted to be 0.85 eV at 0 K. Such a discrepancy indicates a stronger confinement in the valence band of the PbSe core, and this observation agrees well with the blueshift in the absorption and emission spectra measured in the Janus structure in comparison with the core-shell nanocrystals.[51] The confinement increase could be explained by a decrease in the core size. This size reduction could, thus, favor the hypothesis that some Pb atoms leave the outermost layers of the PbSe core and diffuse at the surface of the HNCs toward the CdSe facets in order to saturate the oleate ligands there. Another explanation could be related to the formation of a sharp interface that could modify the confinement potential of the PbSe hemisphere, suggesting a complex hybridization of the electronic states between the rocksalt PbSe part and the zinc-blende CdSe part.

V. CONCLUSION

We have investigated the line shape of the core levels of oleate-capped PbSe/CdSe heteronanocrystals. From the modification of the core-level spectra under the photon beam, a transformation of the chemical structure has been found, that is corroborated with the structural transformation observed by TEM: UV irradiations as well as heating turn PbSe/CdSe core-shell nanocrystals into a Janus structure. Since the photon energy used in these experiments is quite sensitive to the elements at the surface of the nanocrystals, we have shown that photoelectron measurements provide an important insight into the phase transformation of these heteronanocrystals: Not only inorganic atoms rearrange inside the nanocrystals, but also this rearrangement takes place along a reorganization of the ligands that diffuse from Cd surface atoms to saturate the protruding Pb atoms on the PbSe facets. It also leads to an electronic structure that is different from the one obtained for individual PbSe NCs of comparable sizes.

*bruno.grandidier@isen.iemn.univ-lille1.fr

[1] A. Hashimoto, K. Suenaga, A. Gloter, K. Urita, and S. Iijima, Nature (London) **430**, 870 (2004).

[2] L. Liao, H. B. Lu, J. C. Li, C. Liu, D. J. Fu, and Y. L. Liu, Appl. Phys. Lett. **91**, 173110 (2007).

[3] J. Kotakoski, C. H. Jin, O. Lehtinen, K. Suenaga, and A. V. Krasheninnikov, Phys. Rev. B **82**, 113404 (2010).

[4] A. V. Krasheninnikov and F. Banhart, Nat. Mater. **723**, 6 (2007).

[5] F. Börrnert, L. Fu, S. Gorantla, M. Knupfer, B. Büchner, and M. H. Rümmeli, ACS Nano **6**, 10327 (2012).

[6] E. Snoeks, A. Van Blaaderen, T. Van Dillen, C. M. Van Kats, M. L. Brongersa, and A. Polman, Adv. Mater. **12**, 1511 (2000).

[7] L. Sun, A. V. Krasheninnikov, T. Ahlgren, K. Nordlund, and F. Banhart, Phys. Rev. Lett. **101**, 156101 (2008).

[8] S. Dai, J. Zhao, L. Xie, Y. Cai, N. Wang, and J. Zhu, Nano Lett. **12**, 2379 (2012).

[9] M. Meyns, N. G. Bastus, Y. Cai, A. Kornowski, B. H. Juárez, H. Weller, and C. Klinke, J. Mater. Chem. **20**, 10602 (2010).

[10] M. A. Van Huis, A. Figuerola, C. Fang, A. Béché, H. W. Zandbergen, and L. Manna, Nano Lett. **11**, 4555 (2011).

[11] E. Frydman, H. Cohen, R. Maoz, and J. Sagiv, Langmuir **13**, 5089 (1997).

[12] H. Döllefeld, C. McGinley, S. Almousalami, T. Möller, H. Weller, and A. Eychmüller, J. Chem. Phys. **117**, 8953 (2002).

[13] C. Mikó, M. Milas, J. W. Seo, R. Gaál, A. Kulik, and L. Forró, Appl. Phys. Lett. **88**, 151905 (2006).

[14] F. Tao, M. E. Grass, Y. Zhang, D. R. Butcher, J. R. Renzas, Z. Liu, J. Y. Chung, B. S. Mun, M. Salmeron, and G. A. Somorjai, Science **322**, 932 (2008).

[15] H. Borchert, D. V. Talapin, C. McGinley, S. Adma, A. Lobo, A. R. B. de Castro, T. Möller, and H. Weller, J. Chem. Phys. **119**, 1801 (2003).

[16] C. McGinley, H. Borchert, D. V. Talapin, S. Adam, A. Lobo, A. R. B. de Castro, M. Haase, H. Weller, and T. Möller, Phys. Rev. B **69**, 045301 (2004).

[17] K. Huang, R. Demadrille, M. G. Silly, F. Sirotti, P. Reiss, and O. Renault, ACS Nano **4**, 4799 (2010).

[18] W. Heiss, H. Groiss, E. Kaufmann, G. Hesser, M. Böberl, G. Springholz, F. Schäffler, K. Koike, H. Harada, and M. Yano, Appl. Phys. Lett. **88**, 192109 (2006).

[19] J. M. Pietryga, D. J. Werder, D. J. Williams, J. L. Casson, R. D. Schaller, V. I. Klimov, and J. A. Hollingsworth, J. Am. Chem. Soc. **130**, 4879 (2008).

[20] B. De Geyter, Y. Justo, I. Moreels, K. Lambert, P. F. Smet, D. Van Thourhout, A. J. Houtepen, D. Grozsinska, C. de Mello Donega, A. Meijerink, D. Vanmaelelbergh, and Z. Hens, ACS Nano **5**, 58 (2011).

[21] I. Moreels, K. Lambert, D. De Muynck, F. Vanhaecke, D. Poelman, G. Allan, and Z. Hens, Chem. Mater. **19**, 6101 (2007).

[22] K. Lambert, B. De Geyter, I. Moreels, and Z. Hens, Chem. Mater. **21**, 778 (2009).

[23] Y. Justo, I. Moreels, K. Lambert, and Z. Hens, Nanotechnology **21**, 295606 (2010).

[24] J. W. Stouwdam, J. Shan, F. C. J. M. Van Veggel, A. G. Pattantyus-Abraham, J. F. Young, and M. Raudsepp, J. Phys. Chem. C **111**, 1086 (2007).

[25] A. Osherov, M. Shandalov, V. Ezersky, and Y. Golan, J. Cryst. Growth **304**, 169 (2007).

[26] Y. M. Park, R. André, J. Kasprzak, L. Si Dang, and E. Bellet-Amalric, Appl. Surf. Sci. **253**, 6946 (2007).

[27] *Lead Selenide (PbSe) Energy Gap and Band Structure*, edited by O. Madelung, U. Rössler, and M. Schulz, Non-Tetrahedrally Bonded Elements and Binary Compounds I, Landolt-Börnstein, Group III Condensed Matter, Vol. 41C (Springer, Berlin, 1998), p. 1.

[28] T. Dietl, J. Gutowski, B. Hönerlage, F. Matsukara, B. K. Meyerm, and D. Strauch, *New Data and Updates for IV-IV, III-V, II-VI and I-VII Compounds, Their Mixed Crystals and Diluted Magnetic Semiconductors*, edited by U. Rössler, Landolt-Börnstein, New Series, Group III, Condensed Matter, Vol. 44, Pt. D (Springer, Berlin, 2011).

[29] L. Ley, R. A. Pollak, F. R. McFeely, S. P. Kowalczyk, and D. A. Shirley, Phys. Rev. B **9**, 600 (1974).

[30] R. W. Meulenberg, J. R. I. Lee, A. Wolcott, J. Z. Zhang, L. J. Terminell, and T. Van Buuren, ACS Nano **3**, 325 (2009).

[31] H. B. Michaelson, IBM J. Res. Dev. **22**, 72 (1978).

[32] I. Swart, Z. Sun, D. Vanmaekelbergh, and P. Liljeroth, Nano Lett. **10**, 1931 (2010).

[33] G. Allan and C. Delerue, Phys. Rev. B **70**, 245321 (2004).

[34] K. Overgaag, P. Liljeroth, D. Vanmaekelbergh, G. Mahieu, B. Grandidier, G. Allan, and C. Delerue, J. Chem. Phys. **131**, 224510 (2009).

[35] G. Paolucci and K. C. Prince, Phys. Rev. B **41**, 3851 (1990).

[36] J. A. Leiro, K. Laajalehto, I. Katio, and M. H. Heinonen, Surf. Sci. **412/413**, L918 (1998).

[37] F. Maeda, Y. Watanabe, T. Scimeca, and M. Oshima, Phys. Rev. B **48**, 4956 (1993).

[38] W. Chen, A. Kahn, P. Soukiassian, P. S. Mangat, J. Gaines, C. Ponzoni, and D. Olego, Phys. Rev. B **49**, 10790 (1994).

[39] A. J. Nelson, G. Berry, A. Rockett, and D. K. Shuh, Appl. Phys. Lett. **70**, 1873 (1997).

[40] T. Deniozou, N. Esser, T. Schulmeyer, and R. Hunger, Appl. Phys. Lett. **88**, 052102 (2006).

[41] P. John, T. Miller, T. C. Hsieh, A. P. Shapiro, A. L. Wachs, and T.-C. Chiang, Phys. Rev. B **34**, 6704 (1986).

[42] A. Wall, Y. Gao, A. Raisanen, A. Franciosi, and J. R. Chelikowsky, Phys. Rev. B **43**, 4988 (1991).

[43] A. P. J. Stampfl, P. Hofmann, O. Schaff, and A. M. Bradshaw, Phys. Rev. B **55**, 9679 (1997).

[44] S. Evans and J. M. Thomas, J. Chem. Soc., Faraday Trans. 2 **71**, 313 (1975).

[45] A. L. Hagström and A. Fahlman, Phys. Scr. **16**, 432 (1977).

[46] B. A. Orlowski, E. Guziewicz, B. J. Kowalski, T. Story, S. Mickevičius, A. Y. Sipatov, M. Chernyshova, I. N. Demchenko, N. Barrett, M. Taniguchi, A. Kimura, H. Sato, C. A. Sebenne, J. P. Lacharme, R. Medicherla, W. Drube *et al.*, J. Alloys Compd. **362**, 198 (2004).

[47] I. Moreels, B. Fritzinger, J. C. Martins, and Z. Hens, J. Am. Chem. Soc. **130**, 15081 (2008).

[48] V. Petkov, I. Moreels, Z. Hens, and Y. Ren, Phys. Rev. B **81**, 241304(R) (2010).

[49] K. A. Abel, P. A. FitzGerald, T.-Y. Wang, T. Z. Regier, M. Raudsepp, S. Ringer, G. G. Warr, and F. C. J. M. Van Veggel, J. Phys. Chem. C **116**, 3968 (2012).

[50] P. Liljeroth, P. A. Zeijlmans van Emmichoven, S. G. Hickey, H. Weller, B. Grandidier, G. Allan, and D. Vanmaekelbergh, Phys. Rev. Lett. **95**, 086801 (2005).

[51] D. Grodzinska, F. Pietra, M. A. Van Huis, D. Vanmaekelbergh, and C. De Mello, J. Mater. Chem. **21**, 11556 (2011).

[52] T. H. Nguyen, J. Habinshuti, Y. Justo, R. Gomes, G. Mahieu, S. Godey, J. P. Nys, S. Carillo, Z. Hens, O. Robbe, S. Turrell, and B. Grandidier, Phys. Rev. B **84**, 195133 (2011).

[53] A. Ebina, K. Asano, and T. Takahashi, Phys. Rev. B **22**, 1980 (1980).

[54] J. E. Bowen Katari, V. L. Colvin, and A. P. Alivisatos, J. Phys. Chem. **98**, 4109 (1994).

[55] C. J. Vesely and D. W. Langer, Phys. Rev. B **4**, 451 (1971).

[56] V. Leute and R. Schmidt, Z. Phys. Chem. **172**, 81 (1991).

[57] M. A. Pietrzyk, K. Gas, A. Szczerbakow, W. Szuszkiewicz, P. Dziawa, B. A. Orlowski, B. J. Kowalski, and R. L. Johnson, Annual report DESY, 2009 (unpublished).

[58] B. A. Orlowski, M. A. Pietrzyk, A. Szczerbakow, B. J. Kowalski, A. Reszka, K. Gas, W. Szuszkiewicz, V. Domukhovski, S. Mickevicius, R. L. Johnson, S. Thiess, and W. Drube, Annual report DESY, 2010 (unpublished).

[59] S. Bals, M. Casavola, M. A. Van Huis, S. Van Aert, K. J. Batenburg, G. Van Tendeloo, and D. Vanmaekelbergh, Nano Lett. **11**, 3420 (2011).

[60] M. Casavola, M. A. Van Huis, S. Bals, K. Lambert, Z. Hens, and D. Vanmaekelbergh, Chem. Mater. **24**, 294 (2012).

[61] M. A. Van Huis, L. T. Kunneman, K. Overgaag, Q. Xu, G. Pandraud, H. W. Zandbergen, and D. Vanmaekelbergh, Nano Lett. **8**, 3959 (2008).

[62] W. Heiss, E. Kaufmann, M. Böberl, T. Schwarzl, G. Springholz, G. Hesser, F. Schäffler, K. Koike, H. Harada, M. Yano, R. Leitsmann, L. E. Ramos, and F. Bechstedt, Physica E (Amsterdam) **35**, 241 (2006).

[63] M. Law, J. M. Luther, Q. Song, B. K. Hugues, C. L. Perkins, and A. J. Nozik, J. Am. Chem. Soc. **130**, 5974 (2008).